Assessing subsidence rates and paleo water-depths for Tahiti reefs using U-Th chronology of altered corals

Alexander L. Thomas[a,*], Kazuhiko Fujita[b], Yasufumi Iryu[c, 1], Edouard Bard[d], Guy Cabioch[e, †], Gilbert Camoin[d], Julia E. Cole[f], Pierre Deschamps[d], Nicolas Durand[d], Bruno Hamelin[d], Katrin Heindel[g, 2], Gideon M. Henderson[a], Andrew J. Mason[a], Hiroki Matsuda[h], Lucie Ménabréaz[d], Akitoshi Omori[i], Terry Quinn[j, 3], Saburo Sakai[k], Tokiyuki Sato[l], Kaoru Sugihara[m], Yasunari Takahashi[c], Nicolas Thouveny[d], Alexander W. Tudhope[n], Jody Webster[o, 4], Hildegard Westphal[g, 5], Yusuke Yokoyama[k, p, q],

* *Corresponding Author: E-mail, alext@earth.ox.ac.uk; Tel, +44 (0)1865 272047; Fax* +44 (0)1865 272072

a. *Department of Earth Sciences, Oxford University, South Parks Road, Oxford, OX1 3AN, UK*
b. *Department of Physics and Earth Sciences, University of the Ryukyus, Okinawa 903-0213, Japan*
c. *Institute of Geology and Paleontology, Graduate school of Science, Tohoku University, Sendai 980-8578, Japan*
d. *CEREGE (UMR 6635), Aix-Marseille Université, CNRS, IRD, Collège de France, Europole de l'Arbois, BP80, 13545 Aix-en-Provence, France*
e. *Research Unit "Paleotropique" Institut de Recherche pour le Développement BP A5 98848 Nouméa Cedex New Caledonia France*
f. *Geosciences Department University of Arizona 1040 East 4th Street Tucson AZ 85721 USA*
g. *MARUM, Department of Geosciences, University of Bremen, Leobener Strasse, 28359 Bremen, Germany*
h. *Department of Earth Sciences, Faculty of Science Kumamoto University 2-39-1, Kurokami Kumamoto 860-8555 Japan*
i. *Institute of Geosciences, Shizuoka University, Shizuoka, 422-8529 Japan*
j. *College of Marine Science University of South Florida 140 7th Avenue South MSL 119 St. Petersburg FL 33711 USA*
k. *Institute for Research on Earth Evolution, Japan Agency for Marine-Earth Science and Technology, Yokosuka 237-0061, Japan*
l. *Institute of Applied Earth Sciences, Faculty of Engineering and Resource Science, Akita University, Japan*
m. *Earth System Science, Faculty of Science Fukuoka University 8-19-1, Nanakuma Jonan-ku, Fukuoka 814-0180 Japan*
n. *School of GeoSciences, Grant Institute, University of Edinburgh, Kings Buildings, West Mains Road, Edinburgh EH9 3JW. Scotland, U.K.*
o. *School of Earth Sciences James Cook University of North Queensland Townsville QLD 4811 Australia*
p. *Atmosphere and Ocean Research Institute, 5-1-5, Kashiwanoha, Kashiwa-shi, Chiba 277-8564 Japan*
q. *Department of Earth and Planetary Sciences, University of Tokyo, Tokyo 113-0033, Japan*

1. *Now at: Nagoya University, Department of Earth and Planetary Sciences, Graduate School of Environmental Studies, Nagoya University, Nagoya 464-8601, Japan*
2. *Now at Department for Geodynamics and Sedimentology, University of Vienna Althanstrasse 14, 1090 Vienna, Austria*
3. *Now at: Institute for Geophysics, Jackson School of Geosciences, The University of Texas at Austin, J.J. Pickle Research Campus, Bldg 196 (ROC), 10100 Burnet Rd. (R2200), Austin, TX 78758-4445, U.S.A.*
4. *Now at: School of Geosciences, The University of Sydney, NSW 2006, Australia*
5. *Now at: Leibniz Center for Tropical Marine Ecology, Fahrenheitstraße 6, 28359 Bremen, Germany*

†. Deceased. Guy Cabioch passed away during the submission of this manuscript. We wish to recognize the contributions Guy made, not only to the IODP expedition to Tahiti, but also more widely as a carbonate geologist. His presence in the coral reef community will be missed.

Abstract

We present uranium-thorium chronology for a 102 m core through a Pleistocene reef at Tahiti (French Polynesia) sampled during IODP Expedition 310 "Tahiti Sea Level". We employ total and partial dissolution procedures on the older coral samples to investigate the diagenetic overprint of the uranium-thorium system. Although alteration of the U-Th system cannot be robustly corrected, diagenetic trends in the U-Th data, combined with sea level and subsidence constraints for the growth of the corals enables the age of critical samples to be constrained to marine isotope stage 9. We use the ages of the corals, together with $\delta^{18}O$ based sea-level histories, to provide maximum constraints on possible paleo water-depths. These depth constraints are then compared to independent depth estimates based on algal and foraminiferal assemblages, microbioerosion patterns, and sedimentary facies, confirming the accuracy of these paleo water-depth estimates. We also use the fact that corals could not have grown above sea level to place a maximum constraint on the subsidence rate of Tahiti to be 0.39 mka^{-1}, with the most likely rate being close to the existing minimum estimate of 0.25 mka^{-1}.

Keywords: paleo water-depth; Tahiti, IODP Expedition 310; island subsidence; coral; U-Th; open system.

1 Introduction

1.1 Paleo water-depth reconstructions

Estimation of the overlying depth of water is crucial for the reconstruction of past sea levels from geological deposits (typically coral reefs or marine sediments). Ideally a narrow range of possible paleo water-depth, coupled with accurate uplift/subsidence correction, can be combined with a chronological constraint to produce an accurate and precise sea level history. This approach has succeeded in producing archives of sea level from a variety of localities (Bard et al., 1996; Chappell and Polach, 1991; Peltier and Fairbanks, 2006). These records have benefited from relatively shallow paleo water-depths reducing the potential for uncertainty in the correction from water-depth estimate. Where water-depth was thought to be larger, however, accurately recording changes in sea level is more problematic. Also, producing a calibration of fossil assemblage to paleo water-depth involves the study of modern environments of deposition (Hopley, 1986, Montaggioni and Faure, 1995, Cabioch et al., 1999, Humblet et al., 2009, Hongo and Kayanne, 2010) or the examination of fossil material from locations, and times, for which past sea level is well constrained (Montaggioni, 2005). In addition, changes in water transparency, e.g. as an effect of changed trophic conditions, introduce a telescoping effect on biotic assemblages, in particular corals, used for the reconstruction of past sea levels (Heindel et al., 2009a, b). Changes of the water-depths at which assemblages are related through time will therefore also cause sea level estimates to be in error if the calibration is not appropriate.

Often estimates of paleo water-depth are made from material for which some age control already exists (eg Thomas et al., 2009), therefore some bias may be introduced from the expectation of how

89 sea level changed during the time that the material represents. Two recent papers (Fujita et al.,
90 2010; Iryu et al., 2010) have made independent estimates of paleo water-depth (bathymetric ranges)
91 from the same drill core through a carbonate reef, sampled during Integrated Ocean Drilling
92 Program (IODP) Expedition 310 "Tahiti Sea Level". These two sets of estimates are based on
93 benthic foraminifera (Fujita et al., 2010) and non-geniculate coralline algal assemblages (Iryu et al.,
94 2010), and were made without radiometric age control. The addition of age control provided by U-
95 Th measurements of fossil corals from Hole IODP-310-M0005D, coupled with comparison to
96 "known" sea level history, provided the opportunity to check both the robustness of these paleo
97 water-depth estimates as well as their validity back in time. In addition paleo water-depth estimates
98 may be assessed, from post-LGM (Last Glacial Maximum) material, were good chronological and
99 sea level information was available, in an example where water depth was inferred from the basis of
100 the photic levels recorded by microbioerosion patterns (Heindel et al. 2009a, b).
101
102 *1.2 Subsidence rate*
103
104 Volcanic islands emplaced onto oceanic lithosphere are typically found to be subsiding owing
105 principally to the effect of mass loading of the island depressing the underlying oceanic lithosphere
106 (Watts and Zhong, 2000), along with a small component of subsidence related to the cooling and
107 thickening of the oceanic lithosphere itself. At Tahiti – on 74 Ma crust (Muller et al., 2008) – this
108 secondary component equates to only 0.0088 mka^{-1} (Stein and Stein, 1992), the bulk of the
109 subsidence resulting from the loading of the island during the main shield building phase of
110 volcanism 1.4 - 0.87 Ma (Hildenbrand et al. 2004). Constraining this rate of subsidence is not only
111 important for our understanding of crust-mantle dynamics (Moore, 1970; Courtney and White,
112 1986; Zhong and Watts, 2002) but is also crucial for the accurate reconstruction of past sea levels

113 from relative sea level indicators on such ocean islands (Bard et al., 1996; Muhs et al., 2002; Szabo et
114 al., 1994). Modern geodetic measurements (Fadil et al., 2010) of vertical island movement suffer
115 from relatively short baselines and also form the potential of anthropogenically driven ground
116 movement (Bird, 1993) biasing results. Geodetic measurements of subsidence at Tahiti typically
117 have uncertainties that are of comparable size to the rate measured (0.3 ± 0.4 mka^{-1} (Fadil et al.,
118 2010)). It is therefore advantageous to estimate subsidence over longer time periods, giving a time-
119 averaged subsidence rate.
120
121 Previous estimates of long-term subsidence at Tahiti have provided minimum estimates based on
122 radiometric dating of, now submerged, sub-aerial lava flows of 0.21 and 0.25 mka^{-1} (LeRoy, 1994;
123 Bard et al., 1996). Short-term subsidence rate has been estimated from the position of Holocene
124 shoreline deposits and is significantly lower at 0.15 mka^{-1} (Pirazzoli et al., 1985), although other
125 higher Holocene estimates of 0.3 - 0.4 mka^{-1} (Montaggioni, 1988) have also been made. Large
126 uncertainties of these Holocene estimates arise from the relatively short baselines of the
127 measurements, amplifying uncertainties in paleo-sea level and water-depth used in subsidence rate
128 calculations. Here we use the additional constraints provided by U-Th dating of much older fossil
129 corals to provide a maximum estimate of subsidence rate to better constrain the history of the
130 island.
131
132 *1.3 Core description*
133 More than 630 m of cores were recovered during IODP Expedition 310 (Expedition 310 Scientists,
134 2007), and were described sedimentologically within the standardized procedure of the IODP
135 onshore Science Party (Camoin et al., 2007). The deglacial coral reef framework is heavily encrusted
136 by microbialites, in many cases preceded by coralline algal crusts (Seard et al., 2011; Westphal et al.,

2010). Most of the reef framework is therefore preserved in growth position. Hole IODP-310-M0005D was drilled at 17º 45.9915'S 149º 33.0476'W in 59.63 m water-depth on the south-western side of Tahiti, and reached down to 161.8 mbsl (meters below modern sea level, defined as lowest astronomical tide). A total of 36 core sections were recovered from this hole (Fig. 1). Although the conventional core recovery was 64.86% (Camoin et al. 2007), accounting for void space, 97.35% of the available material was retrieved (Inwood et al., 2008).

The lithology of Hole IODP-310-M0005D is described in detail by Camoin et al. (2007) and the pre last glacial sections are summarised by Fujita et al. (2010) and Iryu et al. (2010). Briefly the hole consists of: The postglacial sequence of coralgal framestone and microbialite of cores 1R-6R, from 91.39 – 82.63 mbsl, which was deposited while sea level rose during the last deglaciation (the chronology will be presented elsewhere Deschamps et al., In Revision, Camoin et al., In Revision). An older sequence of coralgal framestone in cores 7R-8R; a rhodolith floatstone and grainstone in cores 9R-15R; a sandy *Halimeda* floatstone, and packstone in cores 16R-20R; a further sequence of coralgal framestone in cores 20R and 21R; a microbialite sequence in cores 21R-22R; a sequence of sandy grainstones with massive *Porites* corals in cores 23R-28R; a thin sequence of coralgal framestone in core 29R; a rhodolith coral floatstone in core 29R; a thick sequence of coralgal and coral framestones and coral floatstones in cores 30R-35R; a coral floatstone sequence in cores 35R-36R; and the base of the hole is marked by a sandy bioclastic grainstone at the base of core 36R (Fig. 1a). Iryu et al. (2010) identify three distinct horizons within Hole IODP-310-M0005D which represent erosional hiatuses, based on the presence of sharp contacts with evidence of carbonate dissolution in the underlying unit. These unconformities are in cores 21R, 29R, and 36R (Fig. 1a).

2. Analytical techniques

Coral samples were identified as being pristine by visual, and thin section, inspection and by X-ray diffraction to ensure that they were primary aragonite (0.26% calcite detection limit). Approximately 0.3 g sub-samples of coral were cut using a hand-held diamond wheel. These chips were then cleaned by ultra-sonication in 18 MΩcm (Milli-Q) water. For U and Th analysis, samples were weighed into Teflon beakers and spiked with a mixed ^{229}Th:^{236}U spike ((Robinson et al., 2004a), with 0.006% ^{230}Th, 0.02% ^{238}U, 0.004% ^{235}U, and 39 ppt ^{234}U impurities, and calibrated with the HU-1 standard assuming the half lives and U:Th of Cheng et al. 2000). Total dissolution is achieved by drop-wise addition of 7.5N HNO_3 to the sample immersed in Milli-Q water. Once dissolved, any remaining organic material is removed by refluxing in hot 15N HNO_3 followed by an attack in cold aqua regia. The sample is converted to nitrate form by repeated drying and dissolution in 15N HNO_3 before being prepared for anion exchange chromatography to separate U and Th from the sample matrix and each other. The chromatographic separation followed the procedure of Thomas et al., (2006) with volumes scaled to accommodate 2 ml of resin.

To investigate the possibility that deviation from closed system of U and Th is localised to the surfaces of the coral, a leaching approach was taken. To ensure only the surfaces of the corals were leached, a weak acid attack with ascorbic acid (63 μM) was used, incorporating NaEDTA (25 μM) to ensure leached Th was not reabsorbed to the remaining solids, following the procedure of Lomitschka and Mangini (1999), and varying the leaching time from 0.5 to 3 hours. Because the coral used for this partial leaching procedure was of the finely porous genus Porites, it was crushed and passed through a 106 μm sieve (the scale of the theca is approximately 100 μm) so that all of the surfaces of the coral were equally subject to the acid leach. Chips of uncrushed coral were also subjected to the same leaching procedure to test the necessity of the crushing step. Once leached

184 samples were rinsed with Milli-Q water to remove any remaining leachate and NaEDTA, they were
185 then prepared for U-Th analysis in the same way as for unleached samples. Measurement of U and
186 Th from the leachate was not possible due to the difficulty in separating the leached Th and U from
187 the EDTA complexing agent.
188
189 Measurement of U and Th isotopes was by Nu instruments MC-ICP-MS in static mode. U and Th
190 isotopes were measured separately, with ^{234}U and ^{230}Th in an ion counter and all other isotopes in
191 Faraday collectors. Machine biases were corrected for using CRM-145 (for uranium), and an in-
192 house ^{229}Th:^{230}Th:^{232}Th standard (for thorium) (Mason and Henderson 2010), bracketing each
193 sample with 3 standard measurements to also asses instrumental reproducibility. For both U and Th
194 measurements the ^{234}U or ^{230}Th concentration is matched to the standard's so that the intensity of
195 the beam in the ion counter is equal, to negate any possible instrumental biases arising from non-
196 linear collector responses.
197
198 **3. Results**
199
200 Uranium and thorium concentrations and isotope ratios are presented in Table 1, and calculated
201 ages in Table 2. Details of the biological assemblages and inferred paleo-environments are presented
202 in Fujita et al. (2010) (benthic foraminifera) and Iryu et al. (2010) (coralline algae). The results of
203 these two studies are summarized in Fig. 1. The foraminiferal assemblages were analysed from core
204 sections M0005D-26R to 16R and have been interpreted as a shallow water environment
205 (15 ± 15 mbsl) in sections 26R to 23R followed by a deepening upwards sequence in core sections
206 18R to 16R (from 45 ± 15 to 75 ±15 mbsl) (Fig. 1d). Coralline algal assemblages from all of the pre-
207 LGM sections have also been investigated (Iryu et al., 2010). The relative paleo water-depths

interpreted are shallow from section M0005D-36R to 30R, deep in section 29R, shallow in sections 28R to 23R, deep in 22R and 21R, followed by a deepening upwards sequence from 21R to 17R, and then deep water from 17R to 7R (Fig. 1g).

4. Discussion

4.1 Partial dissolution of coral to "remove" open system U-Th contamination

A hypothetical coral sample that incorporated uranium from seawater with a ($^{234}U/^{238}U$) of 1.146±0.005 should follow the closed system evolution path (Fig. 2) as it ages: ($^{230}Th/^{238}U$) increasing as ^{230}Th is produced from decay of ^{234}U, and ($^{234}U/^{238}U$) decreasing as initial excess ^{234}U incorporated from sea water, decays towards secular equilibrium (($^{234}U/^{238}U$) = 1). A range of potential seawater ($^{234}U/^{238}U$) is considered due to the potential for subtle secular variation in the isotopic composition of uranium in seawater (Esat and Yokoyama 2006). Deviation from this path is observed for many fossil corals (e.g. compilation in Henderson (2002) because of open-system behaviour over the history of the fossil. This open system behaviour is the result of gain or loss of any of the isotopes in the ^{238}U-^{230}Th decay chain (^{238}U, ^{234}Th, ^{234}Pa, ^{234}U, or ^{230}Th). Often the gain/loss of ^{234}U and ^{230}Th during open system behaviour is coupled leading to linear arrays of data in ($^{234}U/^{238}U$)-($^{230}Th/^{238}U$) space, for corals which are thought to be of similar age (Gallup et al., 1994). This coupled behaviour has been used to apply corrections to coral U-Th data, which fall away from the hypothetical closed-system evolution path, to calculate open-system ages (Scholz et al., 2004; Thompson et al., 2003; Villemant and Feuillet, 2003). These approaches of correcting for open-system behaviour rely on the data falling on a linear array and the assumption that a single type of coupled ^{234}U-^{230}Th gain/loss has occurred. Data for multiple measurements of coral from

core 24R (Table 1 and Fig. 2) indicate these criteria are not upheld (the measurements show enhanced elevation of $^{230}Th/^{238}U$ without the associated elevated $^{234}U/^{238}U$ typical of coupled addition), and therefore open system correction to these data will not necessarily yield more accurate ages.

The partial dissolution of coral 23R illustrates that successive removal of surface material generally moves the position of the coral towards the closed system age evolution line in $(^{234}U/^{238}U)$-$(^{230}Th/^{238}U)$ space (Fig. 4). This indicates that the sequential dissolution technique may be useful in isolating portions of corals that have not been subject to open system behaviour, by preferential removing the outer surfaces which have been potentially exposed to open system behaviour through interaction of uranium and/or thorium isotopes between the coral and pore fluid. However, the measured values of $(^{234}U/^{238}U)$ and $(^{230}Th/^{238}U)$ for partially dissolved sub samples should not be considered more representative of a closed system, because removal of the outer surface of the coral by partial dissolution is on such a small scale that there will have been recoil exchange between the high ^{234}U and ^{230}Th exterior and the "unaltered" interior (Henderson et al., 2001). The $(^{234}U/^{238}U)$ and $(^{230}Th/^{238}U)$ of the leached samples should not therefore be used to calculate a conventional closed system age. Indeed, some of the leached sub-samples move away from the closed system line, which may represent a more complex heterogeneous alteration of the coral or an artefact of the leaching procedure. That the leached coral U-series data lie close to the closed system evolution path, coupled with constraints based on our knowledge of the subsidence rate of Tahiti and the history of global sea level, an approximation of the age of the coral can be made.

4.2 Refinement of the subsidence rate of Tahiti

A previous estimate of the subsidence rate of Tahiti has been made from a K-Ar age, of 549 ± 11 ka, on a now submerged lava flow, at 114 mbsl (Bard et al., 1996). This placed a minimum constraint on the subsidence rate of 0.207 ± 0.004 mka^{-1}. A faster rate being possible if the lava flow was emplaced substantially above sea level, and lower rate if the lava was emplaced during a period of sea level lowstand. This is in reasonable agreement with an earlier unpublished estimate of 0.25 mka^{-1} (LeRoy, 1994), using similar methodology. A lower, Holocene, subsidence rate of 0.15 mka^{-1} has been inferred from the elevation of corals and beach deposits on Tahiti relative to nearby 'stable' islands (Pirazzoli et al., 1985). This discrepancy between the longer and shorter timescale estimates is not unexpected. The subsidence rate due to the loading of an island on the oceanic lithosphere is time dependent, being most rapid at the time of loading and reducing with time (Watts and Zhong, 2000). In consideration of the longer timeframe, a minimum subsidence rate of 0.25 mka^{-1} is assumed here, based on the expectation that subsidence rate in the Holocene is a minimum constraint on the rates further into the past. Also, that the ages of corals interpreted here are 100s of ka old, similar to the age from which this subsidence rate has been measured, makes this a suitable subsidence assumption.

Constraining the time that corals in M0005D could have grown is possible by considering that the corals could only have grown while sea level was above the position they were in – assuming the corals are found in growth position. Reconstructing the elevation of core M0005D back through time (using a subsidence rate of 0.25 mka^{-1}), comparison with a continuous estimate of sea level (Bintanja and van de Wal, 2008), and the U-Th constraint that M0005D-20R was deposited during the MIS 6-5 transition (Table 2 and Fig. 3), indicates that the only times that core section

M0005D-23R would have been underwater, are: MIS 6.5; MIS 7; MIS 8.5; MIS 9 and MIS 11 (Fig. 3a).

The U-series data for the partial leaching of sample 23R and the multiple measurements of corals from 24R suggests that both corals grew during MIS 9 (Fig. 2). Assuming – as seams reasonable – that seawater ($^{234}U/^{238}U$) remained close to 1.146 (Henderson 2002; Robinson et al., 2004b), these corals appear to have undergone open system behaviour in which there was a significant amount of ^{230}Th addition as well as the possibility of coupled ^{234}U-^{230}Th addition. It is possible that seawater may have been higher during MIS 9, Andersen et al. 2010 suggest it may have been as high as 1.152. If this higher seawater ($^{234}U/^{238}U$) is considered then it suggests this coral has undergone less open-system alteration and hence more confidence that this coral is of MIS 9 age.

An upper limit on the subsidence rate can be determined from this new age estimate: that these corals are of MIS 9 age. If the magnitude of the highstand during MIS 9 is inferred from $\delta^{18}O$ based reconstructions of sea level as 0 mbsl at 325 ka (Bintanja and van de Wal, 2008) or 6 mbsl at 329 ka (Rohling et al., 2009), and the corals are assumed to have grown at sea level, then the subsidence rate would be 0.39 mka^{-1} or 0.36 mka^{-1} respectively. Uncertainty of the magnitude of the highstand of $\pm$10 m or in the timing of the highstand of $\pm$10 ka leads to uncertainty the subsidence rate of 0.03 and 0.01 mka^{-1}, respectively. This is a maximum constraint of the subsidence rate because the corals may not have grown during the absolute maximal sea level highstand, instead growing while sea level was slightly lower as it rose (fell) to(from) the highstand and/or could, as is likely, have grown in a depth of water greater than zero. A paleo water-depth of 15 m, as has been suggested for these corals (Fujita et al., 2010), would reduce the maximum subsidence rate by 0.045 mka^{-1}. These new data therefore provide an absolute maximum constraint on subsidence, over the past 325 ka, of

303 0.39 ± 0.03 mka^{-1}, although it is likely to have been lower, allowing for the depth of water that the
304 corals grew under, and for the possibility that they did not grow at the sea level maximum.
305
306 *4.3 Comparison of paleo water-depth estimates with sea level history and age constraints*
307
308 The age constraints provided by U-Th dating can be used to assess water-depth estimates made
309 from fossil assemblages (Fujita et al., 2010; Iryu et al., 2010). A coral from M0005D-20R-2W has
310 yielded a robust U-Th age (Thomas et al 2009). This coral was broken into two fragments in the
311 core. While the upper fragment (5D8146, Tables 1 and 2) has >1% calcite and the replicate U-Th
312 ages do not agree, the lower fragment (5D8006, Tables 1 and 2) appears to be purely aragonite with
313 replicate ages in agreement at 133.6±1.0 and 133.7±0.4 ka. Although the $(^{234}U/^{238}U)_i$ of this
314 fragment indicates that there has been some open-system behaviour it is reasonable to assume that
315 this coral grew at some time approximately 133-134 ka. The age of this coral, when compared to
316 other sea level records for this interval (Andrews et al., 2007; Esat et al., 1999) and other corals
317 from Tahiti from Hole M0019A-27R to 29R (Thomas et al., 2009) suggest this time was during a
318 millennial scale lowstand which followed a brief period when sea level was higher, and preceded sea
319 level rise towards the interglacial of MIS 5.5.
320
321 Both Fujita et al. (2010) and Iryu et al. (2010) identify an increase of water-depth in the cores
322 immediately above M0005D-20R (cores 19R-16R, Fig. 1), in the case of Fujita et al. from 45-75 m
323 water depth. Although we cannot be certain as to the absolute age of these cores, they have been
324 shown to record the Blake geomagnetic excursion (115-120 ka) (Menabreaz et al., 2009). These
325 water-depth interpretations are, therefore, consistent with the rise in sea level during the
326 penultimate glacial termination, and ultimately representing a deeper water environment while sea

level was high during the MIS 5.5 highstand. Hypothesised ages, positions and hence paleo water-depths of these cores are illustrated by open triangles in Fig. 3. Assuming a subsidence rate of 0.25 mka^{-1} the corals in M0005D-20R-2W were deposited at 84 mbsl. If the MIS 5.5 highstand was ~-8 mbsl (Kopp et al 2009) then the maximum water-depth that could have existed above these corals was 94 m (including 2 m of subsidence from 133 ka to the time of the maximum highstand). If core M0005D-16R is indeed MIS5.5 age then this would imply a water-depth of 83 m (16R is 11 m above 20R in the hole), which is in remarkably good agreement with the paleo water-depth estimation of Fujita et al of 75 ± 15 m. This age constraint therefore indicates that both methods for paleo water-depth estimation are sensitive to increasing water-depth and have accurately recorded the sea level rise over the latter part of the penultimate deglaciation (Termination II).

Further comparisons between the age constraints and the paleo water-depth interpretations can be made in the older sections of Hole M0005D. Iryu et al. (2010) suggest M0005D-23R to 24R, characterized as a sandy bioclastic grainstone with massive *Porites* colonies, is representative of a shallow water environment at the beginning of the penultimate deglaciation which is then punctuated by a sea level reversal (Andrews et al., 2007; Esat et al., 1999; Siddall et al., 2006; Thomas et al., 2009) from deeper water in M0005D-22R to 21R (characterised by bioclastic packstones and microbiolites with encrusting corals) back to shallow water in M0005D-21R to 20R (coralgal framestone consisting of massive Porites). Fujita et al. (2010) also suggest M0005D-23R to 24R is shallow water deposit from the beginning of termination II, but has no data to constrain the water-depth from M0005D 22R-21R. Ages of M0005D-23R to 24R are much older (MIS 9) than is assumed by Fujita et al. (2010) and Iryu et al. (2010). Because there is no direct age control on the core sections 21R and 22R it is entirely possible that the age interpretation of Iryu et al. (2010) is

correct, although it is just as feasible that the material from these core sections was deposited during MIS 7 or 9.

The U-Th data combined with the minimum subsidence rate constraint has shown the M0005D-23R to 24R corals to be of MIS 9 age rather than from the early deglacial of the MIS 6-5 transition. The paleo depth of these corals has been estimated as 15±15 m on the basis of foraminiferal assemblage (Fujita et al., 2010) and also "shallow" (< 20 m water-depth) on the basis of nongenticulate coralline algae (Iryu et al., 2010). A constraint on the maximum possible paleo water-depth available for these corals to grow, based on a minimum subsidence rate of 0.25 mka^{-1} and sea level history is 45 m (Fig. 3). The constraints on subsidence rate (0.25-0.39 mka^{-1}) are however loose enough for this estimate to be as shallow as zero (this is from the construction of the maximum subsidence rate being constrained by the criterion that these corals must have grown below sea level).

A coral from core M0005D-30R has been found to display considerable open system behaviour for U-Th such that an accurate age cannot be determined. It is however interesting to note that using an open-system correction (Thompson et al., 2003), assuming an initial seawater ($^{234}U/^{238}U$) of 1.146, the untreated coral and one of the leached aliquots appear to be of MIS 11 age, although when considering the scatter of the other leached aliquots it is not clear that such an open-system correction is merited (other sub-samples of the same coral suggest an older MIS 13 age (Table 2)). That section 30R is below 23R and 24R infers that it is indeed older than them but it could be that it is from some time in MIS 9 earlier than then, rather than necessarily being as old as MIS 11. The occurrence of erosional features in core sections between 24R and 30R (Fig. 1a and h, and Iryu et al. 2010), however, suggest that there had been a fall in sea level between these to "dated" corals

374 (potentially during MIS 10). This stratigraphic control implies that the older interpretation of MIS
375 11 for section 30R is more likely, although the possibility of millennial scale sea level variability
376 during the MIS 9 highstand being responsible for the erosional features cannot be discounted. The
377 only paleo water-depth estimates for sections 29R-36R are by Iryu et al. (2010), and are all
378 "shallow" except for 29R which displays a rhodolith assemblage characteristic of "deep" water (>
379 50 m water-depth). If the minimum subsidence rate of 0.25 mka^{-1} is considered, and it is assumed
380 that core 29R is of MIS 11 age (based on a tenuous open-system age interpretation, and position
381 below an unconformity assumed to represent MIS 10) then the maximum possible water-depth is
382 ~40 m (Fig. 3). The shallow water depth inferred for 30R therefore may reflect lower sea level
383 during the rise from MIS 12 to MIS 11. If, however, the corals from 29R are from MIS 9 then the
384 maximum available water-depth is ~58 m. Faster rates of subsidence would reduce these available
385 water-depths, therefore if the corals from 29R are representative of deep water then the upper
386 estimate of subsidence rate becomes less likely.
387
388 The robustness of paleo water depth reconstructions can also be assessed from cores covering the
389 last deglaciation, where radiocarbon chronology, the elevation of the samples and knowledge of sea
390 level during the deglaciation can be used to provide "known paleo-bathymetry" to test
391 reconstructions. Here we investigate reconstructions based on microbioerosion patterns. Since light
392 controls the occurrence of phototrophic endoliths, their traces left in corals from different water-
393 depths (microbioerosion patterns) reflect different stages of illumination (photic zones), which can
394 be used to reconstruct paleo water-depths (e.g. Vogel and Marincovich, 2004). At Tahiti, the
395 microbioerosion patterns in Holocene corals sampled in cores from around 115 mbsl
396 (M0024A-11R: 14800 cal. yr BP) to 55 mbsl (M0007B-11R: 9280 cal. yr BP) indicate increasing
397 water-depths (deepening upwards), i.e. a decrease in light levels, which reflects the rising deglacial

sea level (Heindel et al., 2009b). For example at around 115 mbsl microbioerosion in the corals of core M0024A-11R indicates shallow euphotic to deep euphotic conditions, whereas microbioeroders in the immediately overlying red algal crusts and microbialites imply dysphotic conditions, ie. an increace in water-depth. In combination with calibrated AMS 14C ages, which indicate a significant time delay of ~600 years between coral growth and microbialite development (Seard et al., 2011), the significantly changing microbioerosion patterns in the different substrates next to each other reflect the rapid rise in sea level around Meltwater Pulse 1A (Bard et al., 1996; Heindel et al., 2009b). This expected finding therefore adds confidence to paleo water-depth reconstructions based on microbioerosional patterns. Although, as with all paleodepth reconstruction, care must be taken to consider the potential of other environmental factors that may influence the "water depth proxy". For example the potential of water turbidity to condense photic zones and hence bias paleodepth estmates to deeper values (Heindel et al., 2009a, b).

5. Conclusions

Leaching of shallow water corals that display "open system" U-Th behaviour has the potential to remove U and Th added to the coral's surface leaving a residue that is closer to a closed system, however the resulting residue may not be considered to be representative of a closed system.

A minimum subsidence rate constrains the possible ages of sections 23R and 24R to highstands MIS 6.5, 7, 8.5, 9, or 11, and the U-Th data further limits the possible age of corals from these sections to be MIS 9.

This extra age constraint places an absolute upper limit on the subsidence rate of 0.39 mka^{-1}, based on the criteria that the corals could not have grown above sea level. Estimates of paleo

water-depth for older corals suggest that this upper limit may be too high and a subsidence rate more similar to the minimum of 0.25 mka^{-1} may be more appropriate.

Comparison of constraints, provided by U-Th dating and subsidence rate, to estimates of paleo water-depths based on sedimentary facies and foraminiferal/algal/microbioeroding assemblages illustrate the accuracy of the paleo water-depth estimates in the absence of prior knowledge of the age and hence expected water-depth.

Acknowledgements

We would like to thank IODP Expedition 310 Scientists for their efforts during sample collection aboard the DP Hunter, and during core processing at the Bremen Core Repository – for which we would also like to thank the BCR staff for their assistance. We thank also, the organizers of the WHOI/IMAGES/PAGES/PALSEA workshop: "Understanding Future Sea Level Rise: the challenges of dating past interglacials" for informative discussion and constructive criticisms, and two reviewers for their thorough inspection of this manuscript and their constructive comments, which have greatly improved this manuscript.

References

Andersen, M.B., Stirling, C.H., Potter, E.K., Halliday, A.N., Blake, S.G., McCulloch, M.T., Ayling, B.F. and O'Leary, M.J., 2010. The timing of sea-level high-stands during Marine Isotope Stages 7.5 and 9: Constraints from the uranium-series dating of fossil corals from Henderson Island. Geochimica et Cosmochimica Acta, 74(12): 3598-3620.

Andrews, J.E., Portman, C., Rowe, P.J., Leeder, M.R. and Kramers, J.D., 2007. Sub-orbital sea-level change in early MIS 5e: New evidence from the Gulf of Corinth, Greece. Earth and Planetary Science Letters, 259(3-4): 457-468.

Bard, E., Hamelin, B., Arnold, M., Montaggioni, L., Cabioch, G., Faure, G. and Rougerie, F., 1996. Deglacial sea-level record from Tahiti corals and the timing of global meltwater discharge. Nature, 382: 241-244.

Bintanja, R. and van de Wal, R.S.W., 2008. North American ice-sheet dynamics and the onset of 100,000-year glacial cycles. Nature, 454(7206): 869-872.

Bird, E.C.F., 1993. Submerging Coasts: The Effects of a Rising Sea Level on Coastal Environments. Wiley, Chichester, 184 pp.

Cabioch G., Montaggioni L.F., Faure G., Laurenti A. (1999) Reef coralgal assemblages as recorders of paleobathymetry and sea level changes in the Indo-Pacific province. Quaternary Science Reviews, 18: 1681-1695.

Camoin, G., Seard, C., Deschamps, P., Webster, J., Abbey, E., Braga, J.-C., Iryu, Y., Durand, N., Bard, E., Hamelin, B., Yokoyama, Y., Thomas, A.L., Henderson, G.M. and Dussouillez, P., In Review. Reef response to sea-level and environmental changes during the last deglaciation. IODP Expedition 310 "Tahiti Sea Level". Geology.

Camoin, G.F., Iryu, Y., McInroy, D.B. and Expedition 310 Scientists, 2007. Proceedings of the IODP, 310. Integrated Ocean Drilling Program Management International, Inc., Washington, DC.

Chappell, J. and Polach, H., 1991. Post-glacial sea-level rise from a coral record at Huon Peninsula, Papua New Guinea. Nature, 349: 147-149.

Cheng, H., Edwards, R.L., Hoff, J., Gallup, C.D., Richards, D.A. and Asmerom, Y., 2000. The half lives of uranium-234 and thorium-230. Chemical Geology, 169: 17-33.

Courtney, R.C. and White, R.S., 1986. Anomalous Heat-Flow and Geoid across the Cape-Verde Rise - Evidence for Dynamic Support from a Thermal Plume in the Mantle. Geophysical Journal of the Royal Astronomical Society, 87(3): 815-867.

Deschamps, P., Durand, N., Bard, E., Hamelin, B., Camoin, G., Thomas, A.L., Henderson, G.M., Okuno, J. and Yokoyama, Y., In Revision. A dramatic ice sheet collapse at the onset of the Bølling warming at 14.6 kyr. Nature.

Esat, T.M., McCulloch, M.T., Chappell, J., Pillans, B. and Omura, A., 1999. Rapid fluctuations in sea level recorded at Huon Peninsula during the penultimate deglaciation. Science, 283(5399): 197-201.

Esat, T.M. and Yokoyama, Y., 2006. Variability in the uranium isotopic composition of the oceans over glacial-interglacial timescales. Geochimica et Cosmochimica Acta, 70(16): 4140-4150.

Expedition 310 Scientists, 2007. Maraa western transect: Sites M0005–M0007. In: G.F. Camoin, Y. Iryu, D.B. McInroy and Expedition 310 Scientists (Editors), Proceedings of the IODP, 310 Integrated Ocean Drilling Program Management International, Inc., Washington, DC.

Fadil, A., Sichoix, L., Barriot, J.P., Ortega, P. and Willis, P., 2011. Evidence for a slow subsidence of the Tahiti Island from GPS, DORIS, and combined satellite altimetry and tide gauge sea level records. Comptes Rendus Geoscience, 343 (5): 331-341

483 Fujita, K., Omori, A., Yokoyama, Y., Sakai, S. and Iryu, Y., 2010. Sea-level rise during Termination
484 II inferred from large benthic foraminifers: IODP Expedition 310, Tahiti Sea Level. Marine
485 Geology, 271, 1-2, 149-155
486 Gallup, C.D., Edwards, R.L. and Johnson, R.G., 1994. The Timing of High Sea Levels over the Past
487 200,000 Years. Science, 263(5148): 796-800.
488 Glaub, I., Gektidis, M. and Vogel, K., 2002. Microborings from different North Atlantic shelf areas
489 – variability of the euphotic zone extension and implications for paleodepth reconstructions.
490 Courier Forschungsinstitut Senckenberg, 237: 25-37.
491 Heindel, K., Westphal, H., Wisshak, M., 2009a. Bioerosion in the reef framework, IODP
492 Expedition #310 off Tahiti (Tiarei, Mara'a, and Faa'a); Proceedings of the IODP, 310,
493 doi:10.2204/iodp.proc.310.201.2009, 28p.
494 Heindel, K., Wisshak, M. and Westphal, H. 2009b. Microbioerosion in Tahitian reefs: A record of
495 environmental change during the last deglacial sea-level rise (IODP 310). Lethaia, 42: 322-
496 340.
497 Henderson, G.M., 2002. Seawater ($^{234}U/^{238}U$) during the last 800 thousand years. Earth and
498 Planetary Science Letters, 199(1-2): 97-110.
499 Henderson, G.M., Slowey, N.C. and Fleisher, M.Q., 2001. U-Th dating of carbonate platform and
500 slope sediments. Geochimica Cosmochimica Acta, 65(16): 2757-2770.
501 Hildenbrand, A., Gillot. P-Y., and Le Roy, I., 2004. Volcano-tectonic and geochemical evolution of
502 an oceanic intra-plate volcano: Tahiti-Nui (French Polynesia). Earth and Planetary Science
503 Letters, 217 (3-4) 349-265.
504 Hongo C., Kayanne H. 2010 Holocene sea-level record from corals: Reliability of paleodepth
505 indicators at Ishigaki Island, Ryukyu Islands, Japan. Palaeogeography, Palaeoclimatology,
506 Palaeoecology. 287 : 143-151.
507 Hopley D (1986) Coral and reefs as indicators of paleo-sea levels, with special reference to the
508 Great Barrier Reef. In: Van de Plassche O (ed): Sea-level research: a manual for the
509 collection and evaluation of data, Geo Books, Norwich: 195-228.
510 Humblet, M., Iryu, Y. and Nakamori, T., 2009. Variations in Pleistocene coral assemblages in space
511 and time in southern and northern Central Ryukyu Islands, Japan. Marine Geology, 259(1-
512 4): 1-20.
513 Inwood, J., Brewer, T., Braaksma, H. and Pezard, P., 2008. Integration of core, logging and drilling
514 data in modern reefal carbonates to improve core location and recovery estimates (IODP
515 Expedition 310). Journal of the Geological Society, 165: 585-596.
516 Iryu, Y., Takahashi, Y., Fujita, K., Camoin, G., Cabioch, G., Matsuda, H., Sato, T., Sugihara, K., Webster,
517 J.M. and Westphal, H., 2010. Sealevel history recorded in the Pleistocene carbonate sequence in
518 IODP Hole 310-M0005D, off Tahiti. Island Arc, 19(4): 690-706.
519 Kopp, R.E., Simons, F.J., Mitrovica, J.X., Maloof, A.C. and Oppenheimer, M., 2009. Probabilistic
520 assessment of sea level during the last interglacial stage. Nature, 462(7275): 863-867.
521 LeRoy, I., 1994. Evolution des volcans en système de point chaud: île de Tahiti, archipel de la
522 Société (Polynésie française), Paris XI, Orsay.
523 Lisiecki, L.E. and Raymo, M.E., 2005. A Pliocene-Pleistocene stack of 57 globally distributed
524 benthic delta O-18 records. Paleoceanography, 20(1): PA1003.
525 Lomitschka, M. and Mangini, A., 1999. Precise Th/U-dating of small and heavily coated samples of
526 deep sea corals. Earth and Planetary Science Letters, 170: 391-401.
527 Ludwig K.R. 2003. User's Manual for ISOPLOT/Ex 3.00. A Geochronological Toolkit
528 for Microsoft Excel.Berkeley Geochronology Center Special Publication. No. 4. 70 pp.
529 Martinson, D.G., Pisias, N.G., Hays, J.D., Imbrie, J., Moore, T.C. and Shackleton, N.J., 1987. Age dating
530 and the orbital theory of the ice ages: development of a high resolution 0 to 300,000-year

chronostratigraphy. Quaternary Research, 27: 1-29.
Mason, A.J. and Henderson, G.M., 2010. Correction of multi-collector-ICP-MS instrumental biases in high-precision uranium-thorium chronology. International Journal of Mass Spectrometry, 295(1-2): 26-35.
Menabreaz, A., Thouveny, N., Camoin, G., and Lund, S. P., 2010. Paleomagnetic record of the late Pleistocene reef sequence of Tahiti (French Polynesia): A contribution to the chronology of the deposits. Earth and Planetary Science Letters 294, 58–68.
Montaggioni, L.F., 1988. Holocene reef growth history in mid-plate high volcanic islands. Proceedings of the Fifth International Coral Reef Congress., 3, 455-460.
Montaggioni, L.F., 2005. History of Indo-Pacific coral reef systems since the last glaciation; development patterns and controlling factors. Earth-Science Reviews, 71(1-2): 1-75.
Moore, J.G., 1970. Relationship between subsidence and volcanic load, Hawaii. Bulletin of Volcanology, 34(2): 562-576.
Muhs, D.R., Simmons, K.R. and Steinke, B., 2002. Timing and warmth of the Last Interglacial period: new U-series evidence from Hawaii and Bermuda and a new fossil compilation for North America. Quaternary Science Reviews, 21: 1355-1383.
Muller, R.D., Sdrolias, M., Gaina, C. and Roest, W.R., 2008. Age, spreading rates, and spreading asymmetry of the world's ocean crust. Geochemistry Geophysics Geosystems, 9: -.
Parrenin, F., Barnola, J.M., Beer, J., Blunier, T., Castellano, E., Chappellaz, J., Dreyfus, G., Fischer, H., Fujita, S., Jouzel, J., Kawamura, K., Lemieux-Dudon, B., Loulergue, L., Masson-Delmotte, V., Narcisi, B., Petit, J.R., Raisbeck, G., Raynaud, D., Ruth, U., Schwander, J., Severi, M., Spahni, R., Steffensen, J.P., Svensson, A., Udisti, R., Waelbroeck, C. and Wolff, E., 2007. The EDC3 chronology for the EPICA dome C ice core. Climate of the Past, 3(3): 485-497.
Peltier, W.R. and Fairbanks, R.G., 2006. Global glacial ice volume and Last Glacial Maximum duration from an extended Barbados sea level record. Quaternary Science Reviews, 25(23-24): 3322-3337.
Perry, C.T. and Macdonald, I.A., 2002. Impacts of light penetration on the bathymetry of reef microboring communities: implications for the development of microendolithic trace assemblages. Palaeogeography, Palaeoclimatology, Palaeoecology, 186: 101-113.
Pirazzoli, P.A., Montaggioni, L.F., Delibrias, G., Faure, G. and Salvat, B., 1985. Late Holocene sea-level changes in the Society Islands and in the northwest Tuamotu Atolls. In: C. Gabrie, J.L. Toffart and B. Salvat (Editors), Proceedings of the Fifth International Coral Reef Congress. Symposia and Seminars (A), Tahiti.
Robinson, L.F., Belshaw, N.S. and Henderson, G.M., 2004a. U and Th concentrations and isotope ratios in modern carbonates and waters from the Bahamas. Geochimica et Cosmochimica Acta 68, (8): 1777-1789.
Robinson, L.F., Henderson, G.M., Hall, L. and Matthews, I., 2004b. Climatic control of riverine and seawater uranium-isotope ratios. Science, 305: 851-854.
Rohling, E.J. et al., 2009. Antarctic temperature and global sea level closely coupled over the past five glacial cycles. Nature Geoscience, 2: 500-504.
Scholz, D., Mangini, A. and Felis, T., 2004. U-series dating of diagenetically altered fossil reef corals Earth and Planetary Science Letters, 218: 163-178.
Seard, C., Camoin, G., Yokoyama, Y., Matsuzaki, H., Durand, N., Bard, E., Sepulcre, S., and Deschamps, P., 2011. Microbialite development patterns in the last deglacial reefs from Tahiti (French Polynesia; IODP Expedition #310): implications on reef framework architecture. Marine Geology, 279, 63-86.
Siddall, M., Bard, E., Rohling, E.J. and Hemleben, C., 2006. Sea-level reversal during Termination II. Geology, 34(10): 817-820.

579 Stein, C.A. and Stein, S., 1992. A Model for the Global Variation in Oceanic Depth and Heat-Flow
580 with Lithospheric Age. Nature, 359(6391): 123-129.
581 Szabo, B.J., Ludwig, K.R., Muhs, D.R. and Simmons, K.R., 1994. Th-230 Ages of Corals and
582 Duration of the Last Interglacial Sea-Level High Stand on Oahu, Hawaii. Science,
583 266(5182): 93-96.
584 Thomas, A.L., Henderson, G.M., Deschamps, P., Yokoyama, Y., Mason, A.J., Bard, E., Hamelin, B.,
585 Durand, N. and Camoin, G., 2009. Penultimate Deglacial Sea-Level Timing from
586 Uranium/Thorium Dating of Tahitian Corals. Science, 324(5931): 1186-1189.
587 Thomas, A.L., Henderson, G.M. and Robinson, L.F., 2006. Interpretation of the 231Pa/230Th
588 paleocirculation proxy: New water-column measurements from the southwest Indian
589 Ocean. Earth and Planetary Science Letters, 241 493– 504.
590 Thompson, W.G., Spiegelman, M.W., Goldstein, S.L. and Speed, R.C., 2003. An open-system
591 model for U-series age determinations of fossil corals. Earth and Planetary Science Letters,
592 210(1-2): 365-381.
593 Villemant, B. and Feuillet, N., 2003. Dating open systems by the 238U-234U-230Th method:
594 application to quaternary reef terraces. Earth and Planetary Science Letters, 210: 105-118.
595 Vogel, K. and Marincovich Jr., L., 2004. Paleobathymetric implications of microborings in Tertiary
596 strata of Alaska, USA. Palaeogeography, Palaeoclimatology, Palaeoecology, 206: 1-20.
597 Watts, A.B. and Zhong, S., 2000. Observations of flexure and the rheology of oceanic lithosphere.
598 Geophysical Journal International, 142(3): 855-875.
599 Westphal, H., Heindel, K., Brandano, M., Peckmann, J. (2010) Genesis of microbialites as
600 contemporaneous framework components of coral reefs, deglacial of Tahiti (IODP 310);
601 Facies, 56, 337-352.
602 Zhong, S.J. and Watts, A.B., 2002. Constraints on the dynamics of mantle plumes from uplift of the
603 Hawaiian Islands. Earth and Planetary Science Letters, 203(1): 105-116.
604
605
606

Table Captions

Table 1

Uranium and thorium concentrations (expressed in mass per mass) and isotope ratios (expressed as activity ratios, using half lives according to Cheng et al. 2000). *Italics* denote data that have been previously published (Thomas et al., 2009). Uncertainties are based on the reproducibility of standard U and Th solutions, within a measurement session. Superscripts in sub-sample IDs denote where sub-samples have bee taken from the same coral specimen.

Table 2

Sample context and calculated ages. Depth below present sea level in meters (mbsl) that the coral was cored from. % of sample remaining following partial dissolution (100%, represents total dissolution of sample, with no leaching proceedure). Closed system age (before 1950 AD) and ($^{234}U/^{238}U$) at time of coral growth (($^{234}U/^{234}U)_i$), calculated using isoplot software (Ludwig, 2003) and the half lives of (Cheng et al., 2000). Open system ages are calculated using the approach of (Thompson et al., 2003) and assuming ($^{234}U/^{234}U)_i$ of modern seawater at 1.146 (Robinson et al., 2004a). *Italics* denote data that have been previously published (Thomas et al., 2009).

Figure Captions

Figure 1

Graphic log of the Pre-LGM sections of Hole IODP 310 M0005D (a), sedimentology (b and e), foraminifera (c) and nongeniculate coralline algal (f) assemblages with associated paleo water-depth interpretations (d and g respectively). Panels a-g are adapted from Fujita et al. (2010) and Iryu et al. (2010). Core sections on which the U-Th data provide age control (h) are illustrated in black (closed-system U-Th age) and grey (marine isotope stage inferred from combination of open-system U-Th data and minimum subsidence rate), erosional contacts from (a) are re-illustrated in (h). Sea level records based on continuous $\delta^{18}O$ (i): solid line, (Bintanja and van de Wal, 2008) on the LR04 timescale (Lisiecki and Raymo, 2005); dotted line (Rohling et al., 2009) on the EDC3 timescale (Parrenin et al., 2007).

Figure 2

($^{234}U/^{238}U$) relationship with ($^{230}Th/^{238}U$) over time for a hypothetical closed system coral that had ($^{234}U/^{238}U)_i$ of 1.146±0.005 (grey band). Time is marked along the closed system band by marine isotope stages following the numbering system of (Martinson et al., 1987). The darker grey sections of the closed system band are the times when core section 23R was submerged (Fig. 3). Ellipses are the 2σ uncertainties of the U-Th data of this study. The black arrow represents the direction coupled addition of ^{234}U and ^{230}Th would drive MIS 11 corals in a possible mode of open system alteration (Thompson et al., 2003).

Figure 3

Plot of core section reconstructed depth vs. age for (A) 0.25 mka^{-1} and (B) 0.35 mka^{-1}. Core sections are shown in grey and sections which have age control provided by U-Th are highlighted in black. Sea level history is shown as a black solid line (Bintanja and van de Wal, 2008) and black dotted line (Rohling et al., 2009). For the 0.25 mka^{-1} scenario the times when sea level was above the position of core section 23R (and hence the only times during which corals could grow) are illustrated by vertical grey bars. Open triangles highlight hypothesised ages and hence paleo water-depths of core sections M0005D-19R to 16R, that record increasing paleo water-depth during the penultimate deglaciation.

Figure 4

The MIS 9 portion of the closed system band from Fig. 2 with age isochrons (grey lines) marked every 10 ka (the isochrons represent where closed system samples would plot if they had exactly the same age but had different ($^{234}U/^{238}U)_i$ – an impossible scenario for corals which should all have the same ($^{234}U/^{238}U)_i$ because seawater should have homogenous uranium isotopes). The ($^{234}U/^{238}U$) and ($^{230}Th/^{238}U$) are plotted for the sub-samples of corals 23R-2W-0, 37 cm and 30R-1W-119, 135 cm which had been subject to partial dissolution (ellipse size is analytical uncertainty). The darkness of the ellipses indication the amount of the initial sub-sample remained following leaching, lighter shades indicating greater dissolution.

666 **Table 1**

Sub-sample ID	IODP Sample ID 310-M0005D-	^{238}U ppm	2s	^{232}Th ppb	2s	(^{230}Th/^{238}U)	2s	(^{234}U/^{238}U)	2s	(^{232}Th/^{238}U)	2s
5D8146a2[a]	*20R-2W-0, 21*	*3.126*	*0.004*	*0.194*	*0.003*	*0.7866*	*0.0028*	*1.1024*	*0.0008*	*0.0000204*	*0.0000004*
5D8146b[a]	*20R-2W-0, 21*	*2.9457*	*0.0004*	*0.2445*	*0.0004*	*0.8020*	*0.0009*	*1.1007*	*0.0008*	*0.00002717*	*0.00000004*
5D8006a2[b]	*20R-2W-14, 21*	*2.736*	*0.004*	*0.216*	*0.004*	*0.7949*	*0.0029*	*1.1081*	*0.0008*	*0.0000259*	*0.0000005*
5D8006c[b]	*20R-2W-14, 21*	*2.5690*	*0.0008*	*0.08490*	*0.00014*	*0.7902*	*0.0009*	*1.1016*	*0.0008*	*0.000010821*	*0.000000018*
5D7198a[c]	24R-1W-73, 87	2.2911	0.0004	0.04475	0.00016	1.0810	0.0022	1.0686	0.0005	0.000006395	0.000000024
5D7198b[c]	24R-1W-73, 87	2.2922	0.0003	0.04366	0.00016	1.0787	0.0022	1.0684	0.0005	0.000006236	0.000000023
5D7198c[c]	24R-1W-73, 87	3.0441	0.0004	1.4241	0.0023	1.0960	0.0012	1.0600	0.0008	0.0001532	0.0000003
5D8256b1	24R-1W-51, 85	2.618	0.003	0.477	0.008	1.040	0.004	1.0671	0.0008	0.0000597	0.0000011
5D23RTop_ac[d]	23R-2W-0, 37	2.3190	0.0003	0.0771	0.0004	1.0383	0.0019	1.0646	0.0007	0.00001088	0.00000005
5D23RTop_ap[d]	23R-2W-0, 37	1.9876	0.0003	3.745	0.018	1.0364	0.0019	1.0623	0.0007	0.000617	0.000003
5D23RTop_bc[d]	23R-2W-0, 37	2.5846	0.0020	0.1563	0.0007	1.0323	0.0021	1.0593	0.0007	0.00001980	0.00000010
5D23RTop_bp[d]	23R-2W-0, 37	2.5651	0.0009	3.290	0.016	1.0259	0.0019	1.0623	0.0007	0.0004199	0.0000020
5D23RTop_cc[d]	23R-2W-0, 37	2.3938	0.0009	0.161	0.001	1.0291	0.0019	1.0638	0.0007	0.00002209	0.00000011
5D23RTop_cp[d]	23R-2W-0, 37	2.6566	0.0013	1.341	0.006	1.0259	0.0020	1.0613	0.0007	0.0001653	0.0000008
5D23RTop_dp[d]	23R-2W-0, 37	2.4011	0.0012	6.44	0.03	1.0234	0.0020	1.0643	0.0007	0.0008782	0.0000042
TFC 2	24R-1W-27, 33	2.2509	0.0010	0.0688	0.0003	1.0516	0.0020	1.0670	0.0007	0.00001000	0.00000005
TFC 3[e]	30R-1W-119, 135	2.2092	0.0012	0.1592	0.0008	1.0748	0.0021	1.0611	0.0007	0.00002360	0.00000011
5D8668b[e]	30R-1W-119, 135	2.3352	0.0003	0.1449	0.0003	1.0905	0.0013	1.0568	0.0009	0.00002031	0.00000004
5D8668c[e]	30R-1W-119, 135	2.2480	0.0003	0.1383	0.0005	1.0958	0.0014	1.0595	0.0009	0.00002014	0.00000007
5D8668dp[e]	30R-1W-119, 135	2.3745	0.0003	0.2373	0.0006	1.0541	0.0014	1.0541	0.0009	0.00003273	0.00000008

667

668 **Table 2**

Sub-sample ID	mbsl	% Residue	Closed System Age ka BP	2s	(234U/ 238U)i	2s	Open System Age ka BP	2s	% calcite	2s
5D8146a2[a]	*117.52*	*100%*	*132.4*	*0.9*	*1.1489*	*0.0012*	130.7	1.0	*1.9%*	*0.3%*
5D8146b[a]	*117.52*	*100%*	*137.9*	*0.4*	*1.1487*	*0.0011*	136.3	0.8		
5D8006a2[b]	*117.66*	*100%*	*133.6*	*1.0*	*1.1576*	*0.0012*	128.3	1.1	*0.3%*	*0.2%*
5D8006c[b]	*117.66*	*100%*	*133.7*	*0.4*	*1.1483*	*0.0011*	132.4	0.7		
5D7198a[c]	128.24	100%	472	15	1.261	0.011	379	8		
5D7198b[c]	128.24	100%	460	14	1.251	0.009	376	8		
5D7198c[c]	128.24	100%					502	18		
5D8256b1	128.02	100%	338	8	1.174	0.004	318	6	0.2%	0.2%
5D23RTop_ac[d]	125.95	84%	340	4	1.1691	0.0021	324	4		
5D23RTop_ap[d]	125.95	89%	343	5	1.1640	0.0021	329	4		
5D23RTop_bc[d]	125.95	71%	342	5	1.1558	0.0022	334	4		
5D23RTop_bp[d]	125.95	56%	322	4	1.1547	0.0018	315	3		
5D23RTop_cc[d]	125.95	100%	324	4	1.1595	0.0019	315	3		
5D23RTop_cp[d]	125.95	65%	324	4	1.1532	0.0019	318	3		
5D23RTop_dp[d]	125.95	100%	313	4	1.1558	0.0018	306	3		
TFC 2	127.78	100%	364	6	1.1876	0.0028	334	5		
TFC 3[e]	141.98	100%	503	20	1.25	0.01	409	9		
5D8668b[e]	141.98	84%					513	21	0.42%	0.04%
5D8668c[e]	141.98	82%					507	21		
5D8668dp[e]	141.98	75%	432	9	1.183	0.003	399	7		

669

670 Figure 1

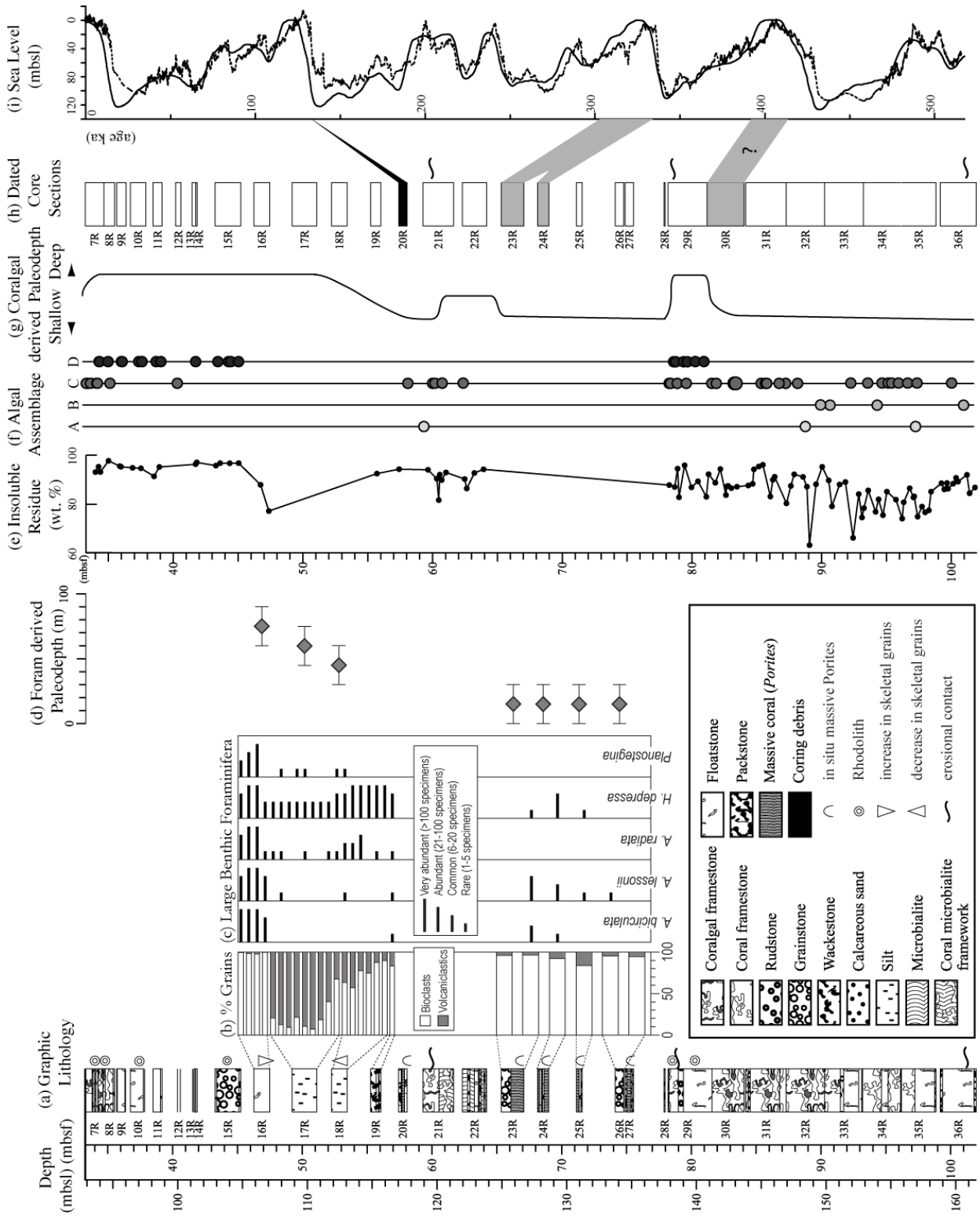

671

672 Figure 2

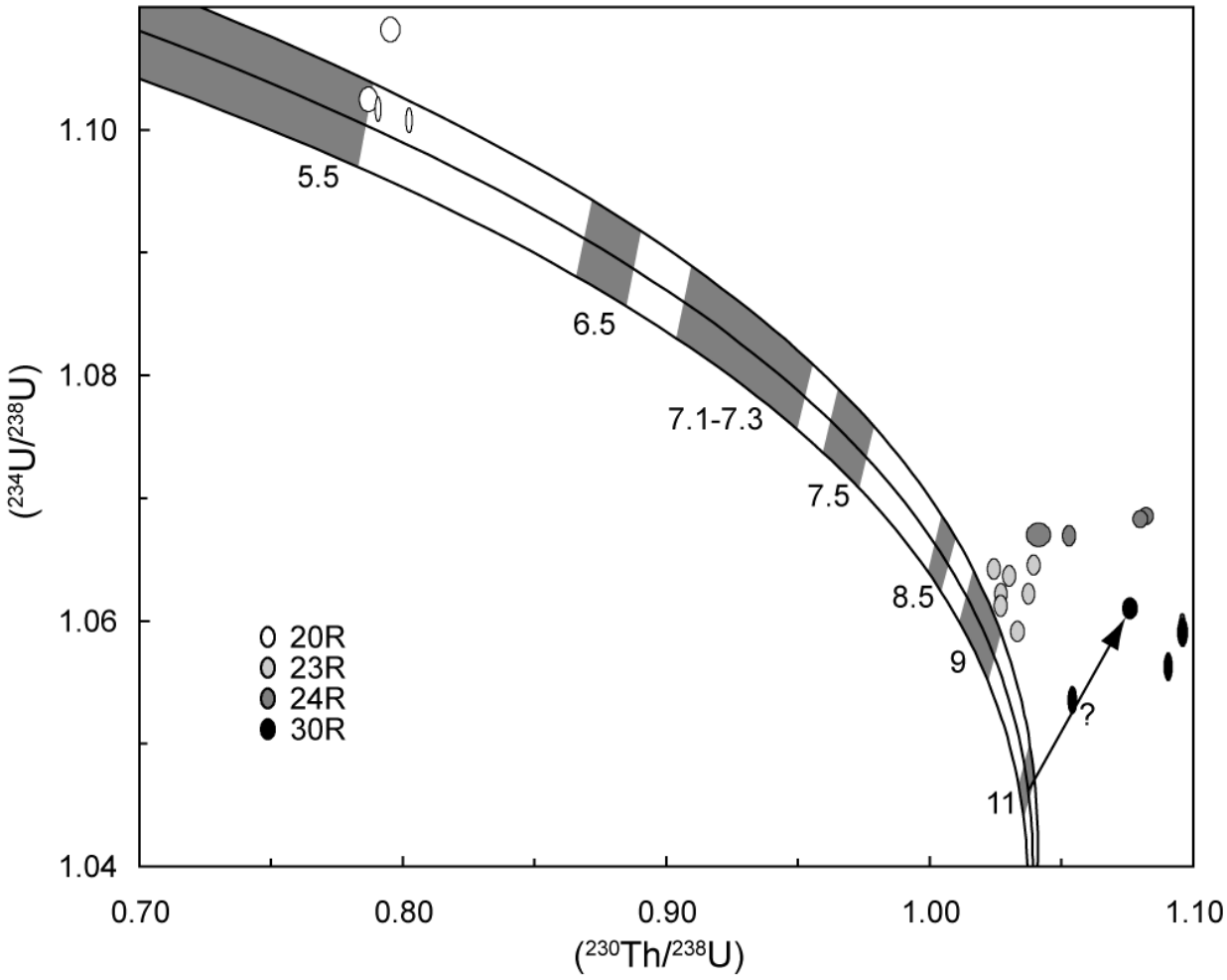

673

674 Figure 3

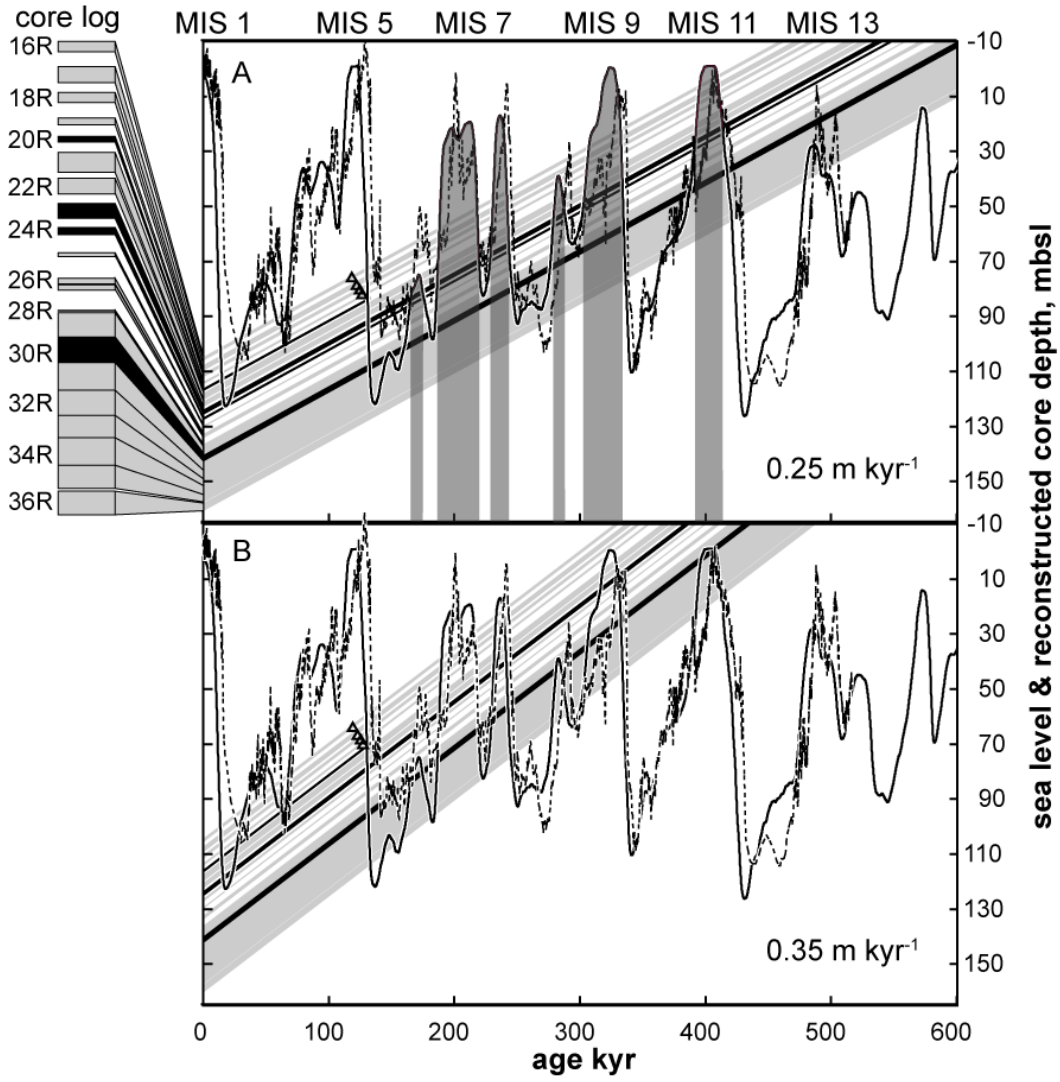

675

676 Figure 4

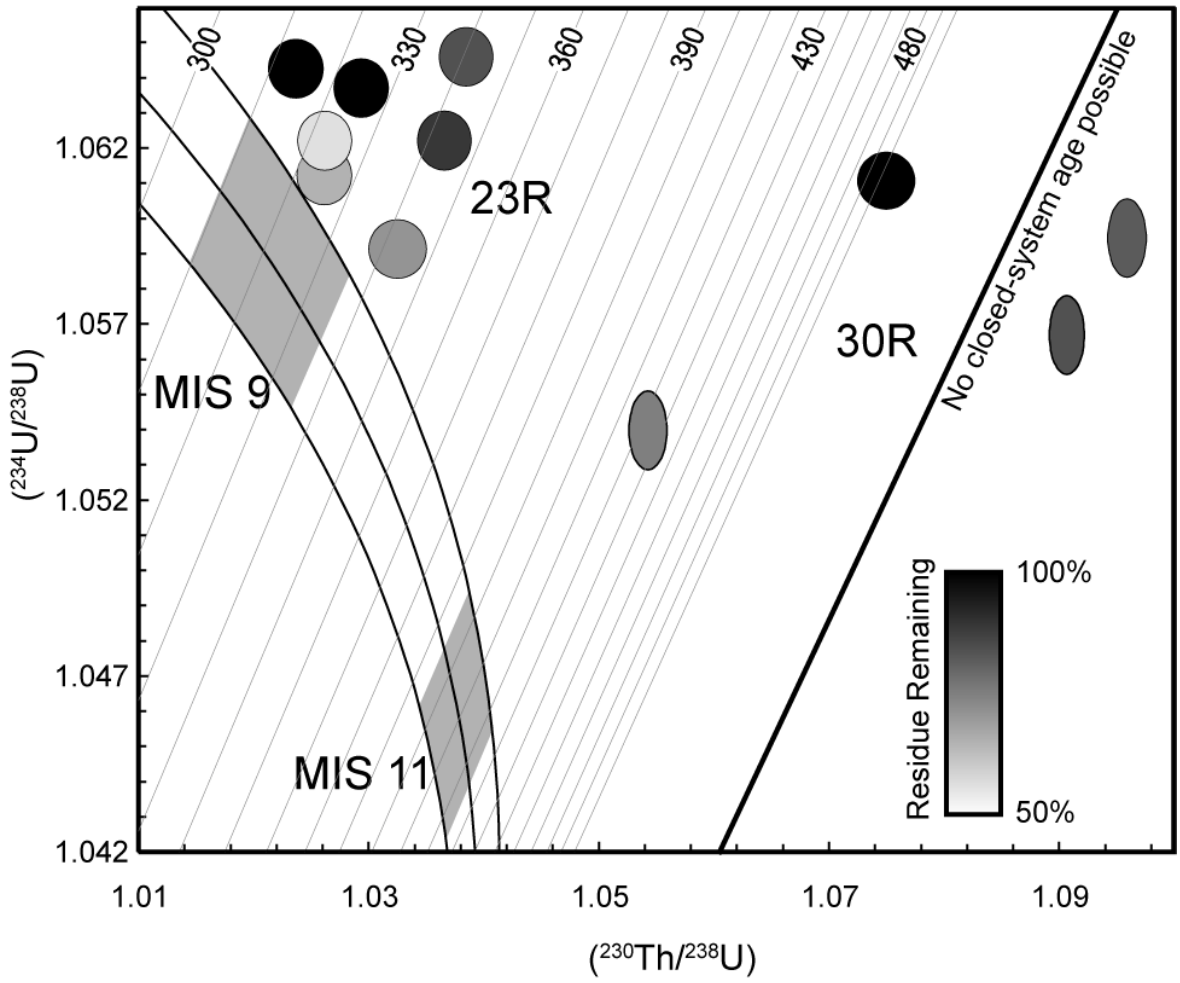

677